Frontiers in Bioscience Landmark

Front. Biosci. (Landmark Ed) **2026**; 31(5): 47016
https://doi.org/10.31083/FBL47016

Original Research

Whole Body Vibration Regulates Neuroinflammation via Sirt3 After Experimental Subarachnoid Hemorrhage

Jian-Meng Lv[1], Juan Liu[1], Wei Li[1], Xuan Wang[1], Mei-Mei Zhang[1], Ya-Juan Pan[1], Tao Wang[1,*]

[1]Department of Neurology, Shaanxi Provincial People's Hospital, 710068 Xi'an, Shaanxi, China
*Correspondence: wangtao_sxrm@163.com (Tao Wang)
Academic Editor: Thomas Heinbockel
Submitted: 29 September 2025 Revised: 19 March 2026 Accepted: 15 April 2026 Published: 26 May 2026

Abstract

Background: Subarachnoid hemorrhage (SAH) represents a severe subtype of hemorrhagic stroke and is associated with unfavorable clinical outcomes. Physical exercise is an effective behavioral intervention that reduces the risk of stroke and preserves neurological function. Whole-body vibration (WBV) is a straightforward form of physical exercise that requires minimal motor skill proficiency. It has positive effects on neuromuscular performance and cardiovascular responses. **Methods**: The present study aims to investigate the potential protective effects of WBV on SAH-induced brain damage and neurological dysfunction in rats. WBV was administered using a vibration platform, with animals stimulation at 30 Hz for two sessions per day over a 30-day period. A modified endovascular perforation technique was employed to establish the *in vivo* SAH model. **Results**: WBV markedly decreased SAH-induced brain edema and inhibited levels of 8-hydroxy-2′-deoxyguanosine (8-OHdG) and MitoSOX, two markers of oxidative stress. Immunostaining analyses demonstrated that WBV significantly attenuated microglial activation (at 24 and 72 h) and astrocytic activation (at 24 h) in the cortical region following SAH. Consistently, WBV markedly inhibited the expression of pro-inflammatory cytokines, including tumor necrosis factor-α (TNF-α) and interleukin-1β (IL-1β), in brain tissue and serum. WBV pretreatment significantly inhibited cortical neuronal apoptosis and downregulated caspase-1 activation at 24 h post-SAH. In addition, WBV activated Sirt3 following SAH, and its protective effects were partially prevented by the Sirt3 inhibitor 3-TYP. **Conclusions**: Our present data indicate that WBV is a clinically potent strategy that protects against the SAH-induced brain damage and neurological dysfunction by regulating Sirt3 and neuroinflammation.

Keywords: subarachnoid hemorrhage; vibration; neuroinflammation; Sirtuin 3

1. Introduction

Subarachnoid hemorrhage (SAH) is a severe form of stroke that most commonly arises from the rupture of intracranial aneurysms, with an estimated prevalence of 3–5% among adults [1]. Although many effective therapeutic strategies have emerged over the last few decades, the prognosis of patients suffering from SAH remains unfavorable due to the unknown mechanisms of early brain injury (EBI) and the subsequent complications, such as cerebral vasospasm. EBI is a complex cascade associated with a transient global ischemia, the increased intracranial pressure (ICP), the activated pro-apoptotic signals and release of blood degradation products, but most of the preclinically investigated agents targeting EBI failed to be translated to the clinic.

Sirtuin 3 (Sirt3), a member of the NAD^+-dependent deacetylase family, is predominantly localized in mitochondria and plays a crucial role in maintaining mitochondrial homeostasis [2]. Emerging evidence suggests that Sirt3 is closely involved in the regulation of oxidative stress and inflammatory responses in the central nervous system [3]. In the context of subarachnoid hemorrhage (SAH), decreased Sirt3 expression has been associated with increased mitochondrial dysfunction, excessive reactive oxygen species (ROS) production, and activation of neuroinflammatory cascades [4,5]. Conversely, activation of Sirt3 has been reported to alleviate early brain injury by suppressing oxidative stress and inhibiting pro-inflammatory signaling pathways [6]. Therefore, Sirt3 is increasingly recognized as a key regulator of neuroinflammation and a potential therapeutic target in SAH.

Regular physical exercise, exemplified by activities such as running, walking, or swimming, are effective behavioral interventions that influences the immune system, neurotrophic factors and cognition. Accumulating evidence have shown that physical exercises not only reduce the risk of stroke, but also preserve neurological function after stroke [7]. Whole-body vibration (WBV) administered at low amplitude and frequency represents an effective exercise intervention with beneficial effects on both the musculoskeletal and nervous systems [8,9]. This intervention is commonly applied in populations presenting with mobility limitations and walking impairments. WBV has been successfully used as a powerful rehabilitative intervention in the management of patients with osteoporosis, osteoarthritis, lumbar disk disease, and Type 2 Diabetes [10,11]. A previous study showed that low amplitude WBV for 4 weeks attenuates brain damage and neurological func-

tion in a MPTP mouse model of Parkinson's disease (PD) [12]. More recently, treatment with 40 Hz WBV for 30 days was shown to reduce brain damage, inhibit neuroinflammation after ischemic stroke in female rats [13]. Furthermore, passive WBV was reported to produce immediate enhancements in attentional capacity and inhibitory mechanisms, even among healthy young individuals demonstrating strong cognitive abilities [14]. Nevertheless, whether WBV can influence brain injury and neurological impairment after SAH remains unclear. Therefore, this study evaluated the effects of WBV on neuroinflammatory responses in a rat model of experimental SAH and explored the possible underlying molecular mechanisms, focusing on Sirt3.

2. Materials and Methods

2.1 Animals

Male Sprague-Dawley rats weighing 280–330 g were procured from the Animal Experimental Center of Shaanxi Provincial People's Hospital. Animals were maintained in a controlled environment (22 °C, 12 h light/dark cycle) with ad libitum access to food and water. Experimental procedures complied with the National Institutes of Health Guide for the Care and Use of Laboratory Animals and adhered to the ARRIVE reporting guidelines [15]. The protocol was reviewed and approved by the Laboratory Animal Ethics Committee of Shaanxi Provincial People's Hospital (Xi'an, China; Approval No. 2021-083). Animals were randomly grouped indiscriminately by means of a table of random numbers. To minimize potential bias, investigators responsible for neurobehavioral assessments, image acquisition and quantification, as well as Western blot analysis were blinded to the group allocation throughout the experiments. Blinding was maintained until completion of data analysis.

2.2 Animal Number and Grouping

A total of 168 male Sprague–Dawley rats were used in this study. Among them, 7 rats died after SAH induction and 11 rats were excluded because of very low SAH grades. Therefore, data from 150 rats were finally included in the analysis and presentation. For all experiments shown in the figures, the sample size was n = 6 animals per group. In the first part of the experiment, rats were randomly assigned to three groups: Sham, SAH, and SAH + WBV. For each group, 6 rats were used for brain water content measurement, 6 rats for immunofluorescence analysis at 24 h, 6 rats for immunofluorescence analysis at 72 h, 6 rats for inflammatory cytokine detection, and 6 rats for neurological function assessment. In the second part of the experiment, rats were divided into four groups: Control, WBV, WBV + 3-TYP, and 3-TYP, with 6 rats per group used for Western blot analysis. In the third part of the experiment, rats were divided into two groups: SAH + WBV and SAH + WBV + 3-TYP. For each group, 6 rats were used for brain water content measurement, 6 rats for immunofluorescence analysis, and 6 rats for inflammatory cytokine detection.

2.3 WBV Induction and SAH Model

WBV stimulation was administered through a vibration apparatus manufactured by Deca Precision Measuring Instruments (Shenzhen, China). Animals were placed individually on the vibration platform and applied with sinusoidal vibration at 30 Hz, administered twice daily (30 min per session) for a total duration of 30 consecutive days according to a previous published paper [16]. During WBV exposure, animals were monitored to ensure they remained in a natural standing position and to minimize stress or fatigue. The *in vivo* SAH model was established using a modified endovascular perforation technique, as previously reported [17]. Briefly, animals were anesthetized with an intraperitoneal injection of pentobarbital sodium solution (10 mg/mL) at a dose of 40–50 mg/kg and maintained at a stable depth of anesthesia throughout the procedure. Under appropriate anesthesia and aseptic conditions, a sharpened monofilament was advanced through the internal carotid artery until resistance was encountered, after which the vessel wall was gently perforated to induce SAH. Successful induction of SAH was confirmed by sudden loss of resistance during perforation and subsequent observation of subarachnoid bleeding. Animals in the sham group underwent identical surgical procedures, but without vessel perforation. To inhibit Sirt3 activation *in vivo*, animals were treated intraperitoneally with 3-TYP, a selective Sirt3 inhibitor (50 mg/kg body weight, suspended in 1% DMSO), once daily for 3 consecutive days prior to SAH induction. This dosing regimen was chosen based on previous studies demonstrating effective inhibition of Sirt3 activity *in vivo*. The pretreatment paradigm was designed to ensure sufficient suppression of Sirt3 signaling before SAH induction and subsequent WBV intervention. SAH severity was evaluated using a previously established SAH grading system at 24 h after model induction. Briefly, the basal surface of the brain was divided into six segments, and each segment was scored from 0 to 3 according to the amount of subarachnoid blood clot: 0, no blood; 1, minimal blood; 2, moderate blood clot with recognizable arteries; and 3, blood clot covering all arteries within the segment. The total SAH grade was calculated as the sum of the six segment scores, ranging from 0 to 18. Animals with very low SAH grades were considered to have unsuccessful modeling and were excluded from subsequent analyses. SAH grading was performed by an investigator blinded to group allocation.

The selection of experimental time points was based on the temporal characteristics of early brain injury (EBI) following SAH. The 24 h time point was chosen to evaluate acute pathological changes, including brain edema, oxidative stress, neuroinflammation, neuronal apoptosis, and Sirt3-related molecular alterations, as these processes are known to peak during the early phase after SAH. Neurological function was assessed at 48 h post-SAH, a time point at which sensorimotor deficits can be reliably and stably detected. In addition, 72 h was selected for the evaluation

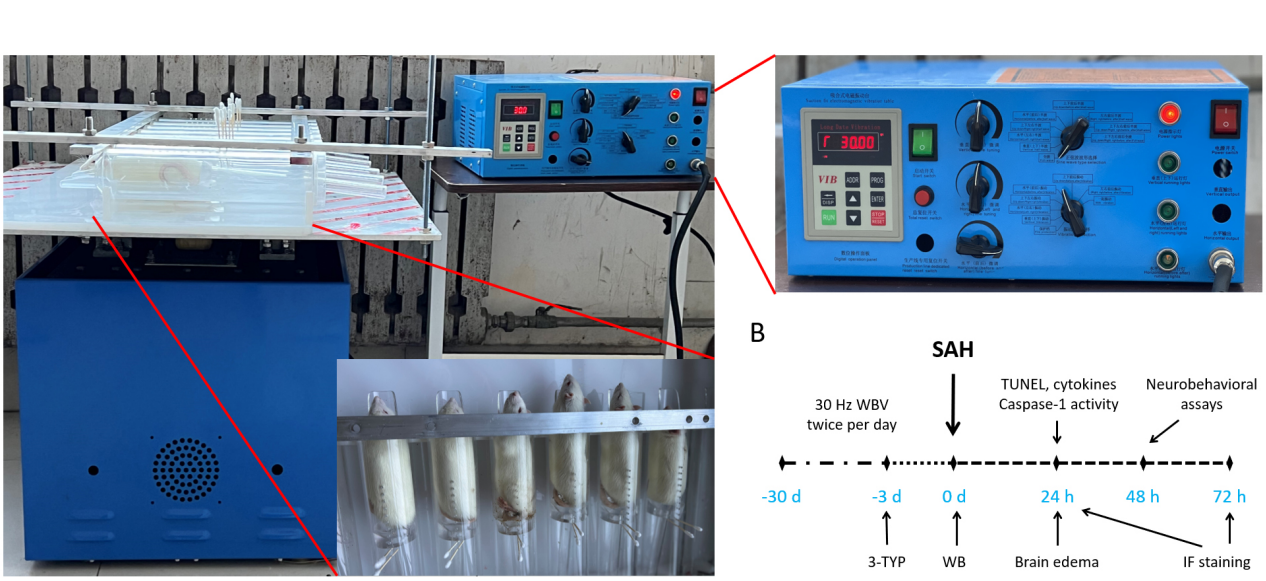

Fig. 1. Equipment and experimental design. (A) The animals were individually fixed on the vibration table, and the vibration parameters were shown in the vibration controller. (B) Schematic illustration of the experimental protocol, including treatments and the timing of different measurements. SAH, subarachnoid hemorrhage.

of glial activation (Iba-1 and GFAP), as neuroinflammatory responses and glial reactivity may persist or evolve beyond the acute phase. This time-course design allowed us to capture both early injury and subsequent neuroinflammatory changes following SAH.

2.4 Brain Water Content

Brain edema was assessed 24 h after SAH induction using the standard wet–dry weight method, as previously reported [18]. Briefly, rats were deeply anesthetized (Isoflurane, 3–5% in oxygen for induction and 1–2% in oxygen for maintenance) and decapitated, and the brains were rapidly removed and separated into the hemispheres, cerebellum, and brainstem on an ice-cold plate. Each tissue sample was immediately weighed to determine the wet weight (WW). The samples were subsequently dried in a thermostatic oven at 100 °C for 24 h until a constant weight was reached, which was recorded as the dry weight (DW). Brain water content in each region was calculated using the following equation: $[(WW - DW) / WW] \times 100\%$.

2.5 Immunofluorescence Staining

Brain tissues embedded in paraffin were sectioned at 4 µm thickness and placed on glass slides. Sections were permeabilized in 0.1% Triton X-100 prepared in PBS for 10 min to facilitate antigen retrieval, and then incubated with 5% bovine serum albumin (BSA) at room temperature for 1 h to minimize nonspecific interactions. Subsequently, sections were incubated overnight at 4 °C with the following primary antibodies: anti-8-OHdG (ab48508, 1:500, Abcam, Shanghai, China), anti-Iba-1 (No.17198, 1:100, Cell Signaling Technology, Shanghai, China), anti-GFAP (No.80788, 1:100, Cell Signaling Technology), and anti-Sirt3 (No.2627, 1:200, Cell Signaling Technology). After three washes with PBS containing 0.05% Tween-20 (PBST, 5 min each), sections were incubated with the appropriate fluorophore-conjugated secondary antibodies (goat anti-rabbit or goat anti-mouse IgG, 1:500; Invitrogen, Carlsbad, CA, USA) at 37 °C for 1 h in the dark. Terminal deoxynucleotidyl transferase dUTP nick end labeling (TUNEL) staining was performed according to the manufacturer's instructions (In Situ Cell Death Detection Kit, Roche, Penzberg, Germany) to evaluate neuronal apoptosis. Following this, the nuclei were stained with 4′,6-diamidino-2-phenylindole (DAPI, 1 µg/mL) for 10 min as a counterstain, and immunofluorescence images were obtained using a Leica SP5 II laser scanning confocal microscope (Leica Microsystems, Wetzlar, Germany). All imaging parameters (laser intensity, gain, exposure time) were kept constant across experimental groups to allow reliable comparisons. Quantitative analysis of immunofluorescence staining was performed using ImageJ software (1.54j, NIH, Bethesda, MD, USA). For each animal, three coronal brain sections at comparable anatomical levels were selected, and at least three non-overlapping fields within the cortical region were randomly captured per section. The region of interest (ROI) was consistently defined within the ipsilateral cortex to ensure comparability across samples. Fluorescence intensity or the number of positive cells was measured and averaged for each section, and subsequently averaged across sections for each animal. All image acquisition parameters were kept constant across groups. Image analysis was performed by investigators blinded to group allocation using coded images, and the results from each animal were used for statistical analysis.

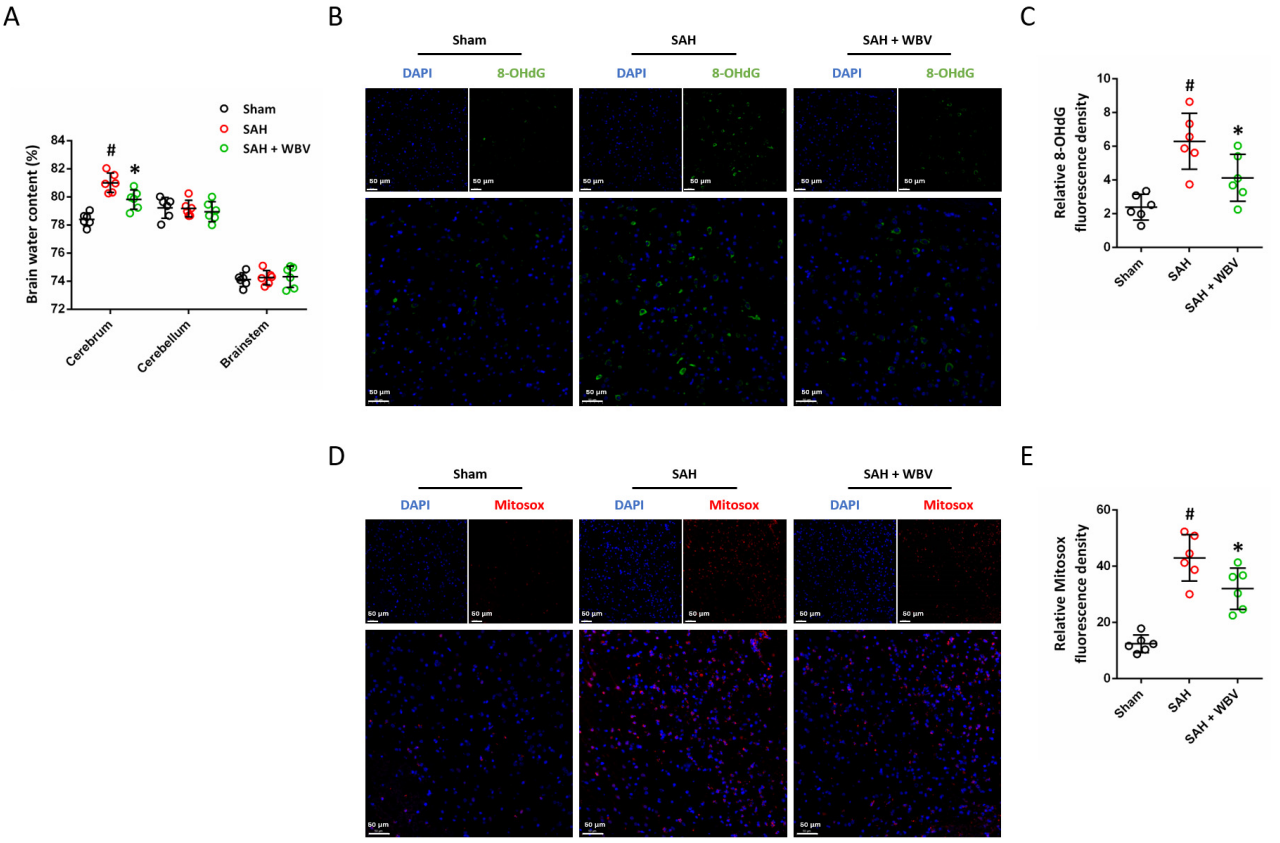

Fig. 2. WBV reduces neuronal injury following SAH. (A) Evaluation of brain water content in different brain regions, including the cerebrum, cerebellum, and brainstem, at 24 h. (B,C) Representative images of 8-OHdG immunostaining in cortex (B) and quantitative analysis (C). (D,E) Typical images of MitoSOX immunostaining in the cortical region (D) and the related quantification (E). Scale bar = 50 µm. n = 6 rats per group. Data are shown as mean ± SD. $^{\#}p < 0.05$ vs. Sham group. $^{*}p < 0.05$ vs. SAH group. WBV, whole body vibration.

2.6 Enzyme-linked Immunosorbent Assay (ELISA)

The concentrations of pro-inflammatory cytokines, including tumor necrosis factor-α (TNF-α, ab46087, abcam), interleukin-1β (IL-1β, ab255730, abcam), and interleukin-6 (IL-6, ab234570, abcam), were quantified using commercially available ELISA kits (Anoric-Bio, Tianjin, China), in accordance with the manufacturer's instructions. Standard curves established with recombinant cytokines were used to determine cytokine levels, which were expressed as pg/mg or pg/mL of protein. All measurements were performed in duplicate to ensure reproducibility, and negative controls were included to exclude nonspecific binding.

2.7 Neurobehavioral Assay

Forty-eight hours after SAH, neurological performance was evaluated by the modified Garcia scale (3–18 points) and the beam balance test (1–6 points). The higher score of the modified Garcia scale suggested better sensorimotor function, whereas the lower score of beam balance test indicated better complex movements and coordination. Neurobehavioral assessments were performed by two independent investigators who were blinded to the experimental groups. Each animal was evaluated twice, and the average score was used for statistical analysis to reduce subjective bias.

2.8 Western Blot

Protein expression was analyzed by Western blot following established methods. In brief, protein samples (30–50 µg per lane) were mixed with loading buffer and heated at 95 °C for 5 min to ensure complete denaturation. The proteins were then resolved using SDS–polyacrylamide gel electrophoresis (SDS–PAGE) and transferred onto polyvinylidene difluoride (PVDF) membranes (Millipore, Billerica, MA, USA). The membranes were blocked for 1 h at room temperature with 5% non-fat milk diluted in Tris-buffered saline containing 0.1% Tween-20 (TBST). After blocking, membranes were incubated overnight at 4 °C with primary antibodies against Sirt3 (1:1000, #2627, Cell Signaling Technology) and GAPDH (1:1000, #5174, Cell Signaling Technology). Following three washes with TBST, HRP-linked secondary antibodies (1:5000; #8889, Cell Sig-

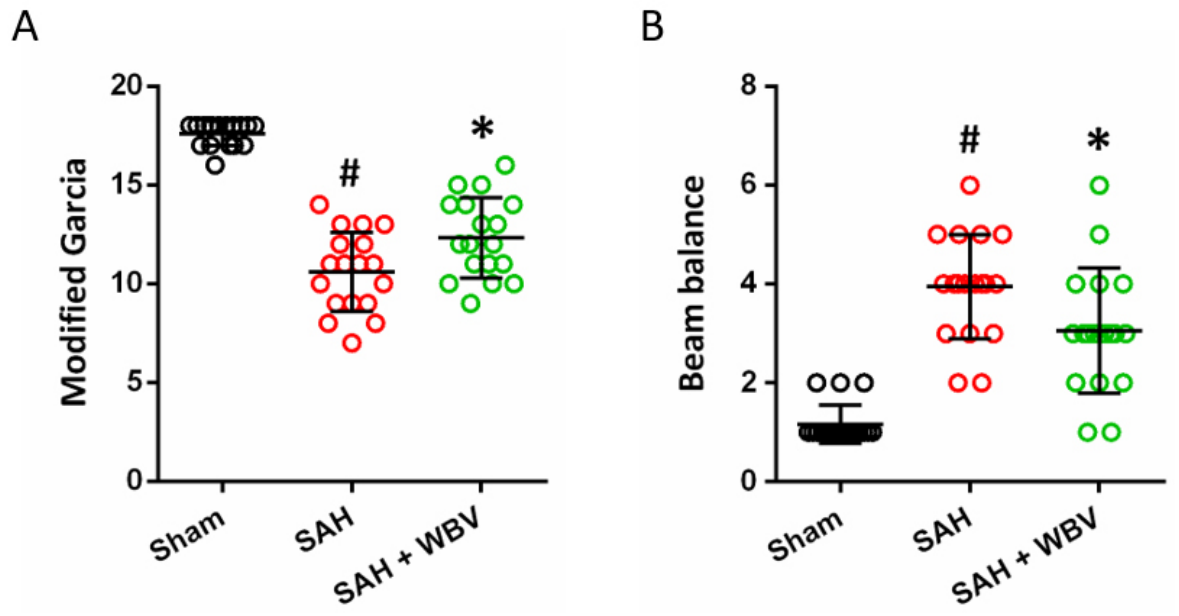

Fig. 3. WBV improves neurological function following SAH. (A) Modified Garcia scale showing sensorimotor function at 48 h. (B) Beam balance test showing complex movements and coordination at 48 h. Data are shown as mean ± SD. n = 6 rats per group. Three repeated measurements from each animal were displayed, resulting in 18 plotted data points per group. $^{\#}p < 0.05$ vs. Sham group. $^{*}p < 0.05$ vs. SAH group.

naling Technology) were applied for 1 h at room temperature. The immunoreactive bands were detected using an enhanced chemiluminescence (ECL) reagent (Thermo Fisher Scientific) and visualized with a ChemiDoc MP Imaging System (Bio-Rad, Hercules, CA, USA). For Western blot analysis, band intensities were quantified using ImageJ software by an investigator blinded to the experimental groups. Each sample was analyzed in at least three independent experiments. The relative expression levels of target proteins were normalized to GAPDH and expressed as fold change compared to the control group.

2.9 MitoSOX Immunostaining

Mitochondrial superoxide production in the cortical region was evaluated using MitoSOX Red staining. Briefly, brain tissues were collected at 24 h after SAH induction, and coronal brain sections at comparable anatomical levels were prepared. After washing with PBS, sections were incubated with MitoSOX Red mitochondrial superoxide indicator working solution (5 µM, Thermo Fisher Scientific, Cat. No. M36008) in the dark at 37 °C for 30 min. Following incubation, the sections were washed three times with PBS to remove excess dye, and nuclei were counterstained with DAPI. Fluorescence images were acquired using a Leica SP5 II laser scanning confocal microscope under identical imaging parameters across all experimental groups.

2.10 Statistical Analysis

Statistical analysis was carried out with SPSS software (version 16.0; IBM Corp., Armonk, NY, USA). All results are expressed as the mean ± standard deviation (SD). The normality of data distribution was first evaluated using the Shapiro–Wilk test, while equality of variances among groups was examined by Levene's test. Differences between two groups were analyzed using Student's *t*-test, with a one-tailed test applied for ratio quantification and a two-tailed test used for the remaining analyses. When more than two groups were compared, statistical differences were assessed by one-way analysis of variance (ANOVA), followed by Tukey's multiple comparison test. Statistical significance was defined as a p value less than 0.05.

3. Results

3.1 Experimental Design and Equipment

As shown in Fig. 1A, the animals were individually fixed on the vibration table, and a vibration apparatus produced by Deca Precision Measuring Instruments (Shenzhen, China) was used to apply WBV. As shown in Fig. 1B, animals received WBV stimulation at 30 Hz for 30 min per session, twice per day, for 30 days, and were then exposed to SAH. Measurements were collected at the specified time intervals.

3.2 WBV Attenuates Brain Damage Following SAH

The influence of WBV on cerebral edema was investigated by measuring brain water content 24 h after SAH induction (Fig. 2A). SAH markedly increased brain water content in the cerebrum, whereas no significant changes were observed in the cerebellum or brainstem. To further assess oxidative DNA damage, immunostaining for 8-

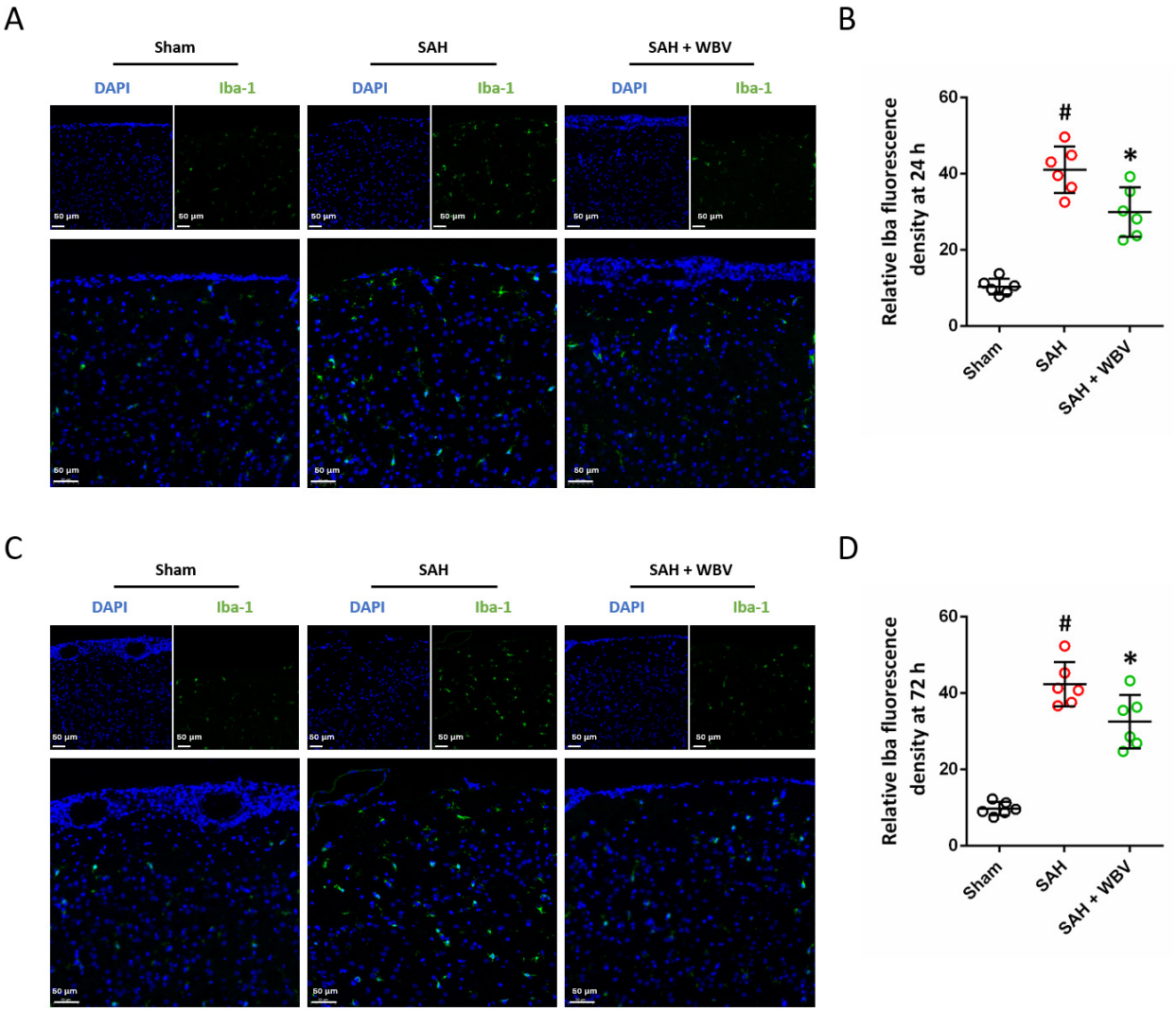

Fig. 4. WBV treatment decreases cortical Iba-1 expression after SAH. (A,B) Typical images of cortical Iba-1 staining (A) and the related quantitative evaluation (B) at 24 h. (C,D) Representative staining of Iba-1 in the cortex (C) with quantitative analysis (D) at 72 h. Scale bar = 50 μm. n = 6 rats per group. Data are shown as mean ± SD. $^{\#}p < 0.05$ vs. Sham group. $^{*}p < 0.05$ vs. SAH group.

OHdG, a well-established biomarker of oxidative nucleic acid modification, was performed (Fig. 2B). SAH resulted in a pronounced increase in 8-OHdG immunoreactivity, which was significantly reduced in animals pretreated with WBV (Fig. 2C). In addition, mitochondrial oxidative stress was evaluated by MitoSOX staining (Fig. 2D). Consistent with the above findings, SAH markedly elevated mitochondrial superoxide levels, while WBV pretreatment significantly suppressed this response (Fig. 2E).

3.3 WBV Attenuates Neurological Dysfunction Following SAH

To assess sensorimotor status, the modified Garcia scale was applied, covering measures of hemiplegia, impaired motor performance, and abnormal postural behavior (Fig. 3A). SAH induction resulted in a significant reduction in Garcia scores, an effect that was effectively abolished by WBV pretreatment. In addition, motor coordination and complex movements were assessed by the beam balance test (Fig. 3B). SAH markedly increased beam balance scores, indicating impaired coordination, and this effect was partially ameliorated by WBV at 48 h post-SAH.

3.4 WBV Inhibits the Expression of Iba-1 Following SAH

Microglial activation in the cortex was evaluated by Iba-1 immunohistochemistry at two time points after SAH, namely 24 h (Fig. 4A) and 72 h (Fig. 4C). Quantitative analysis revealed that SAH markedly increased Iba-1 expression at both time points (Fig. 4B,D). Notably, WBV pretreatment partially attenuated these SAH-induced increases.

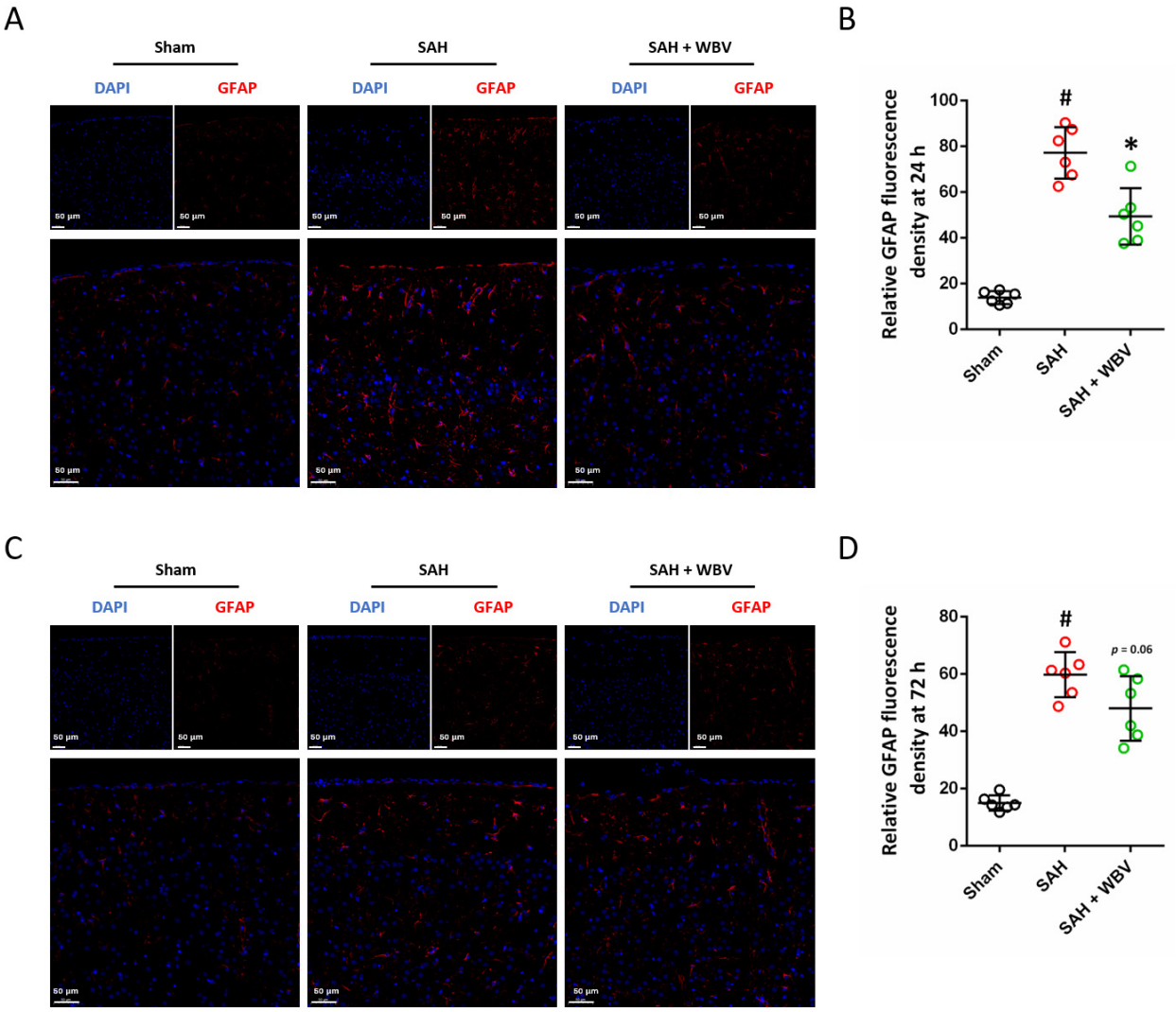

Fig. 5. WBV reduces the expression of GFAP following SAH. (A,B) Typical images showing GFAP staining in the cortex (A) together with the related quantification (B) at 24 h. (C,D) Cortical GFAP staining images (C) and their quantitative evaluation (D) at 72 h. Scale bar = 50 µm. n = 6 rats per group. Data are shown as mean ± SD. $^{\#}p < 0.05$ vs. Sham group. $^{*}p < 0.05$ vs. SAH group. DAPI, 4′,6-diamidino-2-phenylindole; GFAP, Glial fibrillary acidic protein.

3.5 WBV Reduces the Expression of GFAP Following SAH

Cortical astrocyte activation was assessed using GFAP immunostaining at two time points after SAH, namely 24 h (Fig. 5A) and 72 h (Fig. 5C). At 24 h, WBV intervention significantly reduced GFAP expression compared with the SAH group (Fig. 5B). In contrast, GFAP levels at 72 h showed no statistically significant difference between the SAH and SAH + WBV groups (Fig. 5D).

3.6 Effects of WBV on Inflammatory Cytokine Responses After SAH

Brain homogenates were collected at 24 h following SAH, and SAH markedly increased the levels of TNF-α, IL-1β and IL-6, which were reduced by WBV (Fig. 6A). We also detected these cytokines in serum, and we found that the SAH-induced increases in these cytokines were attenuated by WBV, although the expression of IL-6 was not statistically decreased ($p = 0.13$, Fig. 6B).

3.7 WBV Inhibits Neuronal Death Following SAH

The neuronal apoptosis in the cortex was measured by TUNEL staining (Fig. 7A). Quantitative analysis demonstrated that SAH markedly increased the number of TUNEL-positive cells, and this effect was markedly attenuated by WBV pretreatment (Fig. 7B). Consistently, WBV also reduced the SAH-induced elevation of caspase-1 activity, an established marker of inflammatory apoptosis (Fig. 7C).

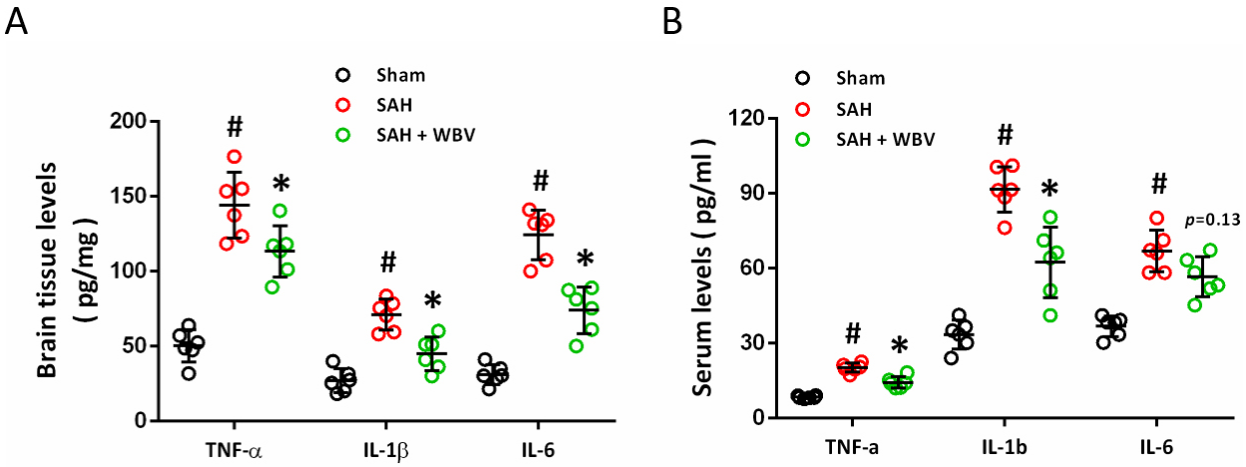

Fig. 6. Effects of WBV on inflammatory cytokine responses after SAH. (A) Quantification of inflammatory cytokines in brain tissue at 24 h assessed by ELISA. (B) ELISA-based quantification of serum inflammatory cytokines at 24 h. n = 6 rats per group. Data are shown as mean ± SD. $^{\#}p < 0.05$ vs. Sham group. $^{*}p < 0.05$ vs. SAH group.

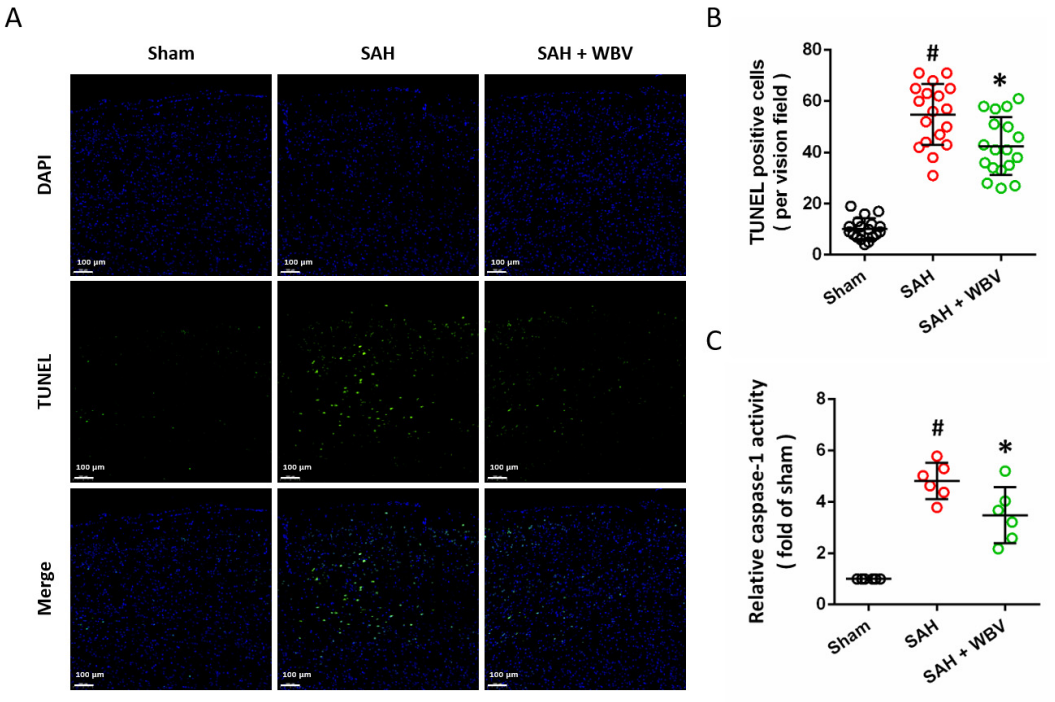

Fig. 7. WBV decreases neuronal death following SAH. (A,B) TUNEL staining in the cortex is presented in representative images (A), with quantitative results shown accordingly (B) at 24 h. (C) Relative caspase-1 activity at 24 h. Scale bar = 100 μm. Data are shown as mean ± SD. n = 6 rats per group. For Fig. 7B, three repeated measurements from each animal were displayed, resulting in 18 plotted data points per group. $^{\#}p < 0.05$ vs. Sham group. $^{*}p < 0.05$ vs. SAH group.

3.8 WBV Protects Against SAH via Activating Sirt3

To better understand the molecular basis of the protective effects associated with WBV, immunohistochemical staining was performed to evaluate Sirt3 expression (Fig. 8A). SAH significantly reduced the Sirt3 protein levels, which was apparently increased by WBV (Fig. 8B). 3-TYP was used to inhibit Sirt3 activity, and we found that WBV-induced Sirt3 expression was reduced by 3-TYP (Fig. 8C). After 3-TYP treatment, the WBV-induced attenuation of 8-OHdG expression following SAH was prevented (Fig. 8D,E). As shown in Fig. 8F,G, a similar result in MitoSOX levels was also observed. In addition, the results of brain water content showed that WBV-induced alleviation of brain water content was significantly reversed by Sirt3 inhibition (Fig. 8H).

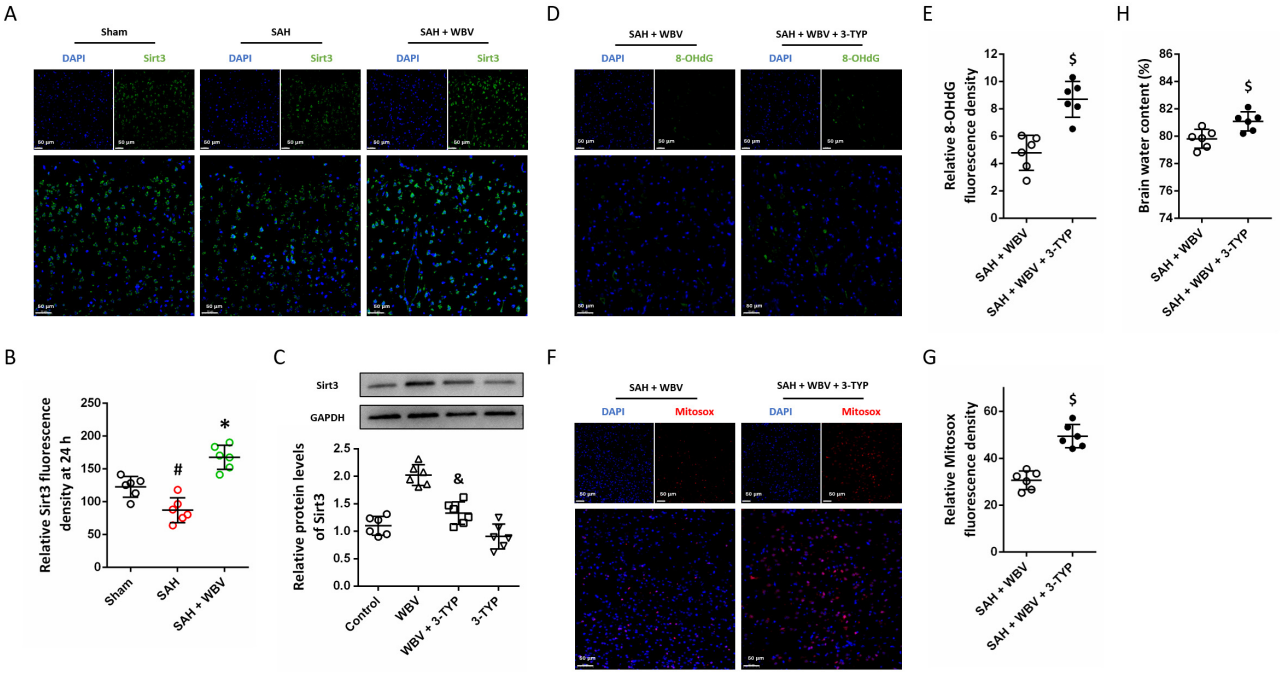

Fig. 8. WBV protects against SAH via activating Sirt3. (A,B) Cortical Sirt3 immunostaining is illustrated in representative images (A), with quantitative evaluation shown in (B). (C) Detection of Sirt3 protein levels by Western blotting. (D,E) Representative cortical images of 8-OHdG staining (D) and their quantitative assessment (E). (F,G) MitoSOX staining in the cortex is presented in representative images (F), with quantitative results shown in (G). (H) Brain edema measurement in cerebrum at 24 h. Scale bar = 50 µm. n = 6 rats per group. Data are shown as mean ± SD. $^{\#}p < 0.05$ vs. Sham group. $^{*}p < 0.05$ vs. SAH group. $^{\&}p < 0.05$ vs. WBV group. $^{\$}p < 0.05$ vs. SAH+WBV group.

3.9 WBV Regulates Neuroinflammation via Activating Sirt3

Next, we further assayed the role of Sirt3 in WBV-induced effects on neuroinflammation. The results of Iba-1 immunostaining showed that WBV-induced inhibition of Iba-1 expression was ablated by 3-TYP (Fig. 9A,B). 3-TYP treatment also increased GFAP expression in cortex following SAH as compared to that in SAH + WBV group (Fig. 9C,D). We repeated the measurements of ELISA in brain tissues (Fig. 9E) and in serum (Fig. 9F), and the results showed that WBV-induced decreases in inflammatory cytokines expression were nullified by Sirt3 inhibition. As shown in Fig. 9G, a similar result in caspase-1 activity was also observed.

4. Discussion

Physical exercise is a neuroprotective strategy for stroke, with beneficial effects against SAH in experimental and clinical settings. WBV is a novel exercise-mimetic intervention that has been applied as an alternative to conventional physical therapy in a variety of disease contexts [19]. In the present study, we examined the effects of WBV on neuronal injury following experimental SAH and identified a regimen of 30 Hz, administered twice daily for 30 consecutive days, as a neuroprotective strategy. We found that (a) WBV reduces SAH-induced brain edema and oxidative stress; (b) WBV attenuates neurological dysfunction induced by SAH; (c) WBV inhibits the activation of astrocytes and microglial cells after SAH; (d) WBV ameliorates neuronal apoptosis and caspase-1 activation after SAH; and (e) WBV protects against SAH and regulates neuroinflammation via activation of Sirt3.

Physical exercise is considered as a mild stressor that follows the typical preconditioning stimulus, and persistent physical exercise promotes general health, especially in the cardiovascular and central nervous system [20]. People who perform regular exercise have a lower risk of stroke, suffer from milder stroke, and get better functional outcomes after stroke [21]. It has been demonstrated that even light exercise, such as walking for 4 h per week, could alleviate stroke severity and improve neurological function [7]. It has been reported that pre-stroke exercise markedly upregulates several protective molecules, including vascular endothelial growth factor (VEGF), nerve growth factor (NGF), brain-derived neurotrophic factor (BDNF), endothelial nitric oxide synthase (eNOS), and hypoxia-inducible factors (HIFs) [22]. More recently, exercise was found to attenuate EBI and reduce cerebral vasospasm after SAH in both experimental and clinical studies [23,24]. WBV is a straightforward form of physical exer-

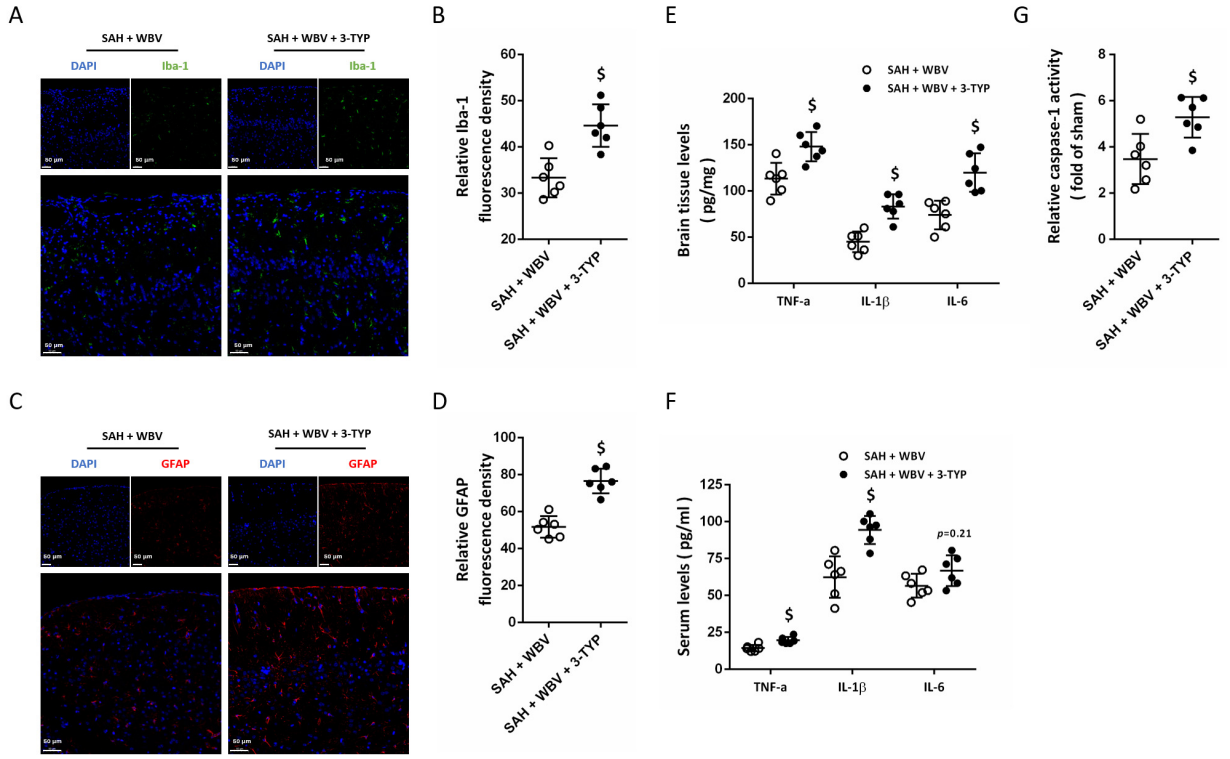

Fig. 9. WBV regulates neuroinflammation via activating Sirt3. (A,B) Cortical Iba-1 immunostaining is presented in representative images (A), with quantitative results shown in (B). (C,D) Representative images illustrating GFAP staining in the cortex (C) and the corresponding quantification (D). (E,F) ELISA results of inflammatory cytokines levels in brain tissues (E) and in serum (F). (G) Relative caspase-1 activity at 24 h. Scale bar = 50 µm. n = 6 rats per group. Data are shown as mean ± SD. $^{\$}p < 0.05$ vs. SAH+WBV group.

cise that requires minimal motor skill proficiency, with positive effects on neuromuscular performance and cardiovascular responses. However, the effects of WBV on neuronal injury and neurological function after stroke are controversial, partly because of the discrepancies in WBV parameters, including frequencies, intensities and number of exercise sessions [25,26]. In the present study, preconditional WBV exercise for 30 days was demonstrated to be neuroprotective against SAH, as indicated by decreased brain water content, inhibited neuroinflammation, decreased neuronal death and preserved neurological function. Our results add some evidence of WBV-induced protection in hemorrhagic stroke.

WBV may trigger diverse physiological responses in the human body, a complex and dynamic system, with outcomes largely determined by vibration frequency, amplitude, and exposure time [27]. Mechanosensitive receptors, including the Meissner's corpuscles, exhibit preferential sensitivity to vibration frequencies within the 30–40 Hz range, while the whole body demonstrates greatest sensitivity across the 1–50 Hz spectrum [28]. Moreover, distinct anatomical regions, such as the thoracic and abdominal cavities as well as the brain, resonate in response to WBV, with vibration at 5 Hz producing greater discomfort relative to other frequencies [29]. However, exposure to WBV at 30 Hz has been reported to exert beneficial acute effects on cognitive function in healthy young adults [14]. In previously published papers on stroke, the frequency of WBV ranged from 1 to 50 Hz, among which most positive results were obtained from WBV at 20–30 Hz [25]. Thus, WBV at 30 Hz was chosen for this study. In addition, the position of the subjects is also important, and squat and sitting with hips and knees fixed were commonly used. In our experiments, rats were individually put into polyethylene tubes that fixed on the vibration table, and the direction of the horizontal vibration (left-right) could not be altered by the slight movement of the animal's body (Fig. 1A). Furthermore, WBV twice per day for 30 days was chosen here, and our pre-experiment data showed that WBV twice per day for 20 days had no positive effects (data not shown). Pang *et al.* [30] showed that WBV training 3 days per week for 8 weeks induced improvements on knee spasticity in stroke patients, and significant increases in the isometric knee extension strength were found when 35–45 Hz WBV training were performed for at least 6 weeks [31]. In addition, Cognitive performance has been found to improve in mice and humans following 5 weeks of WBV exposure at 30 Hz [9]. Our findings, which align with earlier studies, indicate that WBV at 30 Hz administered twice daily for 30 days, preserves neurobehavioral performance in rats following SAH.

Perhaps a more homogeneous group of patients with more severe neurological dysfunction could benefit more from WBV [32], and more experiments are needed to compare different WBV protocols.

The immune inflammatory system of the brain is complex, and can be differently regulated by the resident inflammatory cells, such as microglia and astrocytes, as well as the peripheral inflammatory cells, including monocytes and neutrophils. The activation of neuroinflammation and followed pro-apoptotic cascades is considered as an important mechanism underlying EBI after SAH, and some anti-inflammatory drugs, such as steroids, statins, and nonsteroidal anti-inflammatory drugs (NSAIDs), have been investigated in clinical trials [33]. GFAP serves as a specific marker of astrocytes, and elevated GFAP expression has been reported in rat models of SAH [34]. Atangana *et al*. [35] showed that intracerebral activated microglia contribute to secondary brain injury after experimental SAH. In congruence, our immunostaining data suggested that the enhanced expression of Iba-1 and GFAP were observed at 24 and 72 h after SAH. The activated astrocyte Ca^{2+} signaling promotes the conversion of blood vessels from a diastolic to a vasoconstrictive state, while activated microglia promotes the production of inflammatory cytokines [36]. Elevated levels of inflammatory cytokines, including IL-1, IL-6, and TNF-α, have been reported to be related to the prognosis of SAH patients [37]. In this study, the WBV-induced protection was accompanied by the reduced expression of Iba-1 and GFAP, indicating the role of anti-inflammatory mechanism in our observations.

Originally identified in studies of calorie restriction (CR), sirtuins represent a family of class III histone deacetylases implicated in the regulation of longevity [38,39]. In mammals, seven isoforms (Sirt1–Sirt7) have been characterized, with Sirt3 being predominantly localized to mitochondria. Sirt3, a deacetylase localized in mitochondria, is enriched in metabolically active tissues like the kidney, heart, liver, and brain and contributes to the regulation of multiple mitochondrial activities [3,40]. Accumulating evidence have shown that Sirt3 plays a key role in neurological diseases, ranging from acute insults such as brain ischemia and intracerebral hemorrhage to neurodegenerative illnesses characterized by chronic progression, such as Alzheimer's disease (AD) and Parkinson's disease (PD) [41,42]. In the experimental SAH model induced by endovascular perforation in rats, the decreased expression of Sirt3 mRNA and protein were found to be associated with increased reactive oxygen species (ROS) [43]. Wu *et al*. [6] also showed that SAH significantly decreased Sirt3 expression from 3 to 72 h in C57BL/6 J male mice. In congruent, our data indicated that cortical expression of Sirt3 was decreased by SAH. It was shown that inhibition of Sirt3 activation via its upstream regulator PGC-1α aggravates oxidative stress following experimental SAH in mice [44]. In addition, treatment with honokiol, the pharmacological agonist of Sirt3, was shown to protect against SAH-induced early brain injury via activating AMPK cascades [6]. In the present study, we found that WBV significantly increased Sirt3 expression following SAH. Furthermore, treatment with the Sirt3 inhibitor 3-TYP markedly reversed the WBV-induced protection, as well as its regulation of neuroinflammation. It is shown that swimming exercise could increase Sirt3 expression [45], and the exercise-mediated amelioration of metabolic disorders has been associated with the upregulation of Sirt3 [46]. Thus, WBV-induced protection against SAH might be mediated by Sirt3 activation.

This study has several limitations. First, microglial and astrocytic activation after SAH was evaluated by measuring the expression of Iba-1 and GFAP. However, microglia can polarize into pro-inflammatory M1 and anti-inflammatory M2 phenotypes, while astrocytes may differentiate into A1 (pro-inflammatory) or A2 (anti-inflammatory) subtypes. Additional investigations focusing on these phenotypic changes would provide deeper insight into the anti-inflammatory mechanisms of WBV. In addition, the vibration frequency and amplitude were measured at the surface of the vibration platform, which does not necessarily reflect the exact mechanical stimuli transmitted to the brain. The precise vibration parameters experienced by the animals' brains could therefore not be determined directly. Future studies employing more advanced measurement techniques, such as devices capable of recording vibration signals closer to the brain, or vibrators attached directly to the animals' heads, may help clarify the brain-specific effects of WBV. Furthermore, although we observed that Sirt3 expression was reduced after SAH and restored by WBV, and pharmacological inhibition using 3-TYP partially reversed the protective effects of WBV, the measurement of Sirt3 protein levels does not necessarily reflect its enzymatic activity. Moreover, more specific approaches, such as genetic knockdown of Sirt3 (e.g., siRNA) or direct assessment of Sirt3 deacetylase activity, were not performed in the present study. Therefore, the precise role of Sirt3 activity in mediating the neuroprotective effects of WBV requires further investigation in future studies.

5. Conclusion

Taken together, the results suggest that a 30-day WBV preconditioning regimen at 30 Hz provides neuroprotective benefits after experimental SAH, including reduced brain damage, diminished neuroinflammatory responses, and improved neurological function. These effects are likely linked to Sirt3 activation and its downstream influence on neuroinflammation.

Availability of Data and Materials

The datasets used or analyzed during the current study are available from the corresponding author on reasonable request.

Author Contributions

Conceptualization was done by TW and JML; investigation (including the performance of experiments and acquisition of data) was carried out by TW, YJP, XW, and MMZ; data collection and organization were conducted by WL and JL; original draft was written by JML; review and editing were performed by TW. All authors contributed to editorial changes in the manuscript. All authors read and approved the final manuscript. All authors have participated sufficiently in the work and agreed to be accountable for all aspects of the work.

Ethics Approval and Consent to Participate

All experimental procedures involving animals were undertaken in accordance with the National Institutes of Health guidelines and received approval from the Animal Care and Use Committee of Shaanxi Provincial People's Hospital (No. 2021-083).

Acknowledgment

Not applicable.

Funding

This study has been funded by the Shaanxi Province Natural Science Foundation Research Program (No.2021JM-554 and No.2022JM-587).

Conflicts of Interest

The authors declare no conflicts of interest.

References

[1] Etminan N, Rinkel GJ. Unruptured intracranial aneurysms: development, rupture and preventive management. Nature Reviews. Neurology. 2016; 12: 699–713. https://doi.org/10.1038/nrneurol.2016.150.

[2] Šešelja K, Šimunić E, Sobočanec S, Podgorski II, Pinterić M, Hadžija MP, *et al*. SIRT3-Mediated Mitochondrial Regulation and Driver Tissues in Systemic Aging. Genes. 2025; 16: 1497. https://doi.org/10.3390/genes16121497.

[3] Hong C, Wei Y, Wang Y, Lv G, Dong X, Huang X. The mechanism and therapeutic potential of SIRT3 in central nervous system diseases: a review. Frontiers in Pharmacology. 2025; 16: 1652296. https://doi.org/10.3389/fphar.2025.1652296.

[4] Rehman AS, Kumar P, Parvez S. Dopamine-D2-agonist targets mitochondrial dysfunction via diminishing Drp1 mediated fission and normalizing PGC1-α/SIRT3 pathways in a rodent model of Subarachnoid Haemorrhage. Neuroscience. 2025; 564: 60–78. https://doi.org/10.1016/j.neuroscience.2024.11.028.

[5] Chen T, Wang Y, Wang YH, Hang CH. The Mfn1-βIIPKC Interaction Regulates Mitochondrial Dysfunction via Sirt3 Following Experimental Subarachnoid Hemorrhage. Translational Stroke Research. 2022; 13: 845–857. https://doi.org/10.1007/s12975-022-00999-5.

[6] Wu X, Luo J, Liu H, Cui W, Feng D, Qu Y. SIRT3 protects against early brain injury following subarachnoid hemorrhage *via* promoting mitochondrial fusion in an AMPK dependent manner. Chinese Neurosurgical Journal. 2020; 6: 1. https://doi.org/10.1186/s41016-019-0182-7.

[7] Hafez S, Eid Z, Alabasi S, Darwiche Y, Channaoui S, Hess DC. Mechanisms of Preconditioning Exercise-Induced Neurovascular Protection in Stroke. Journal of Stroke. 2021; 23: 312–326. https://doi.org/10.5853/jos.2020.03006.

[8] Seidel H, Heide R. Long-term effects of whole-body vibration: a critical survey of the literature. International Archives of Occupational and Environmental Health. 1986; 58: 1–26. https://doi.org/10.1007/BF00378536.

[9] Boerema AS, Heesterbeek M, Boersma SA, Schoemaker R, de Vries EFJ, van Heuvelen MJG, *et al*. Beneficial Effects of Whole Body Vibration on Brain Functions in Mice and Humans. Dose-response: a Publication of International Hormesis Society. 2018; 16: 1559325818811756. https://doi.org/10.1177/1559325818811756.

[10] Kitamoto T, Saegusa R, Tashiro T, Sakurai T, Yokote K, Tokuyama T. Favorable Effects of 24-Week Whole-Body Vibration on Glycemic Control and Comprehensive Diabetes Therapy in Elderly Patients with Type 2 Diabetes. Diabetes Therapy: Research, Treatment and Education of Diabetes and Related Disorders. 2021; 12: 1751–1761. https://doi.org/10.1007/s13300-021-01068-0.

[11] Verschueren SMP, Roelants M, Delecluse C, Swinnen S, Vanderschueren D, Boonen S. Effect of 6-month whole body vibration training on hip density, muscle strength, and postural control in postmenopausal women: a randomized controlled pilot study. Journal of Bone and Mineral Research: the Official Journal of the American Society for Bone and Mineral Research. 2004; 19: 352–359. https://doi.org/10.1359/JBMR.0301245.

[12] Zhao L, He LX, Huang SN, Gong LJ, Li L, Lv YY, *et al*. Protection of dopamine neurons by vibration training and up-regulation of brain-derived neurotrophic factor in a MPTP mouse model of Parkinson's disease. Physiological Research. 2014; 63: 649–657. https://doi.org/10.33549/physiolres.932743.

[13] Raval AP, Schatz M, Bhattacharya P, d'Adesky N, Rundek T, Dietrich WD, *et al*. Whole Body Vibration Therapy after Ischemia Reduces Brain Damage in Reproductively Senescent Female Rats. International Journal of Molecular Sciences. 2018; 19: 2749. https://doi.org/10.3390/ijms19092749.

[14] Regterschot GRH, Van Heuvelen MJG, Zeinstra EB, Fuermaier ABM, Tucha L, Koerts J, *et al*. Whole body vibration improves cognition in healthy young adults. PloS One. 2014; 9: e100506. https://doi.org/10.1371/journal.pone.0100506.

[15] Kilkenny C, Browne WJ, Cuthill IC, Emerson M, Altman DG. Improving bioscience research reporting: the ARRIVE guidelines for reporting animal research. PLoS Biology. 2010; 8: e1000412. https://doi.org/10.1371/journal.pbio.1000412.

[16] Chen T, Liu WB, Ren X, Li YF, Li W, Hang CH, *et al*. Whole Body Vibration Attenuates Brain Damage and Neuroinflammation Following Experimental Traumatic Brain Injury. Frontiers in Cell and Developmental Biology. 2022; 10: 847859. https://doi.org/10.3389/fcell.2022.847859.

[17] Duris K, Manaenko A, Suzuki H, Rolland W, Tang J, Zhang JH. Sampling of CSF via the Cisterna Magna and Blood Collection via the Heart Affects Brain Water Content in a Rat SAH Model. Translational Stroke Research. 2011; 2: 232–237. https://doi.org/10.1007/s12975-010-0063-z.

[18] Chen T, Dai SH, Jiang ZQ, Luo P, Jiang XF, Fei Z, *et al*. The AMPAR Antagonist Perampanel Attenuates Traumatic Brain Injury Through Anti-Oxidative and Anti-Inflammatory Activity. Cellular and Molecular Neurobiology. 2017; 37: 43–52. https://doi.org/10.1007/s10571-016-0341-8.

[19] Park YJ, Park SW, Lee HS. Comparison of the Effectiveness of Whole Body Vibration in Stroke Patients: A Meta-Analysis. BioMed Research International. 2018; 2018: 5083634. https://doi.org/10.1155/2018/5083634.

[20] Sanchis-Soler G, Tortosa-Martínez J, Manchado-Lopez C, Cortell-Tormo JM. The effects of stress on cardiovascular dis-

ease and Alzheimer's disease: Physical exercise as a counteract measure. International Review of Neurobiology. 2020; 152: 157–193. https://doi.org/10.1016/bs.irn.2020.01.002.

[21] Deplanque D, Masse I, Libersa C, Leys D, Bordet R. Previous leisure-time physical activity dose dependently decreases ischemic stroke severity. Stroke Research and Treatment. 2012; 2012: 614925. https://doi.org/10.1155/2012/614925.

[22] Otsuka S, Sakakima H, Terashi T, Takada S, Nakanishi K, Kikuchi K. Preconditioning exercise reduces brain damage and neuronal apoptosis through enhanced endogenous 14-3-3γ after focal brain ischemia in rats. Brain Structure & Function. 2019; 224: 727–738. https://doi.org/10.1007/s00429-018-1800-4.

[23] Otsuka S, Setoyama K, Takada S, Nakanishi K, Terashi T, Norimatsu K, *et al*. Preconditioning Exercise in Rats Attenuates Early Brain Injury Resulting from Subarachnoid Hemorrhage by Reducing Oxidative Stress, Inflammation, and Neuronal Apoptosis. Molecular Neurobiology. 2021; 58: 5602–5617. https://doi.org/10.1007/s12035-021-02506-7.

[24] Riordan MA, Kyle M, Dedeo C, Villwock MR, Bauer M, Vallano ML, *et al*. Mild exercise reduces cerebral vasospasm after aneurysm subarachnoid hemorrhage: a retrospective clinical study and correlation with laboratory investigation. Acta Neurochirurgica. Supplement. 2015; 120: 55–61. https://doi.org/10.1007/978-3-319-04981-6_10.

[25] Sañudo B, Taiar R, Furness T, Bernardo-Filho M. Clinical Approaches of Whole-Body Vibration Exercises in Individuals with Stroke: A Narrative Revision. Rehabilitation Research and Practice. 2018; 2018: 8180901. https://doi.org/10.1155/2018/8180901.

[26] Bernardo-Filho M, Taiar R, Sañudo B, Furness T. Clinical Approaches of Whole Body Vibration Exercises. Rehabilitation Research and Practice. 2018; 2018: 9123625. https://doi.org/10.1155/2018/9123625.

[27] Zhou Z, Griffin MJ. Response of the seated human body to whole-body vertical vibration: biodynamic responses to mechanical shocks. Ergonomics. 2017; 60: 333–346. https://doi.org/10.1080/00140139.2016.1179793.

[28] Firmino SG, Duarte MLM, Neves JAB, Viana PAX, de Araújo FSB. Whole body vibration influence on bus fare collectors evaluated by using a brain training mobile app. International Archives of Occupational and Environmental Health. 2021; 94: 495–501. https://doi.org/10.1007/s00420-020-01601-x.

[29] Liang X, Shen H, Shi WD, Ren S, Jiang W, Liu H, *et al*. Effect of axial vertical vibration on degeneration of lumbar intervertebral discs in modified bipedal rats: An in-vivo study. Asian Pacific Journal of Tropical Medicine. 2017; 10: 714–717. https://doi.org/10.1016/j.apjtm.2017.07.014.

[30] Pang MYC, Lau RWK, Yip SP. The effects of whole-body vibration therapy on bone turnover, muscle strength, motor function, and spasticity in chronic stroke: a randomized controlled trial. European Journal of Physical and Rehabilitation Medicine. 2013; 49: 439–450.

[31] Tankisheva E, Bogaerts A, Boonen S, Feys H, Verschueren S. Effects of intensive whole-body vibration training on muscle strength and balance in adults with chronic stroke: a randomized controlled pilot study. Archives of Physical Medicine and Rehabilitation. 2014; 95: 439–446. https://doi.org/10.1016/j.apmr.2013.09.009.

[32] Lau RWK, Yip SP, Pang MYC. Whole-body vibration has no effect on neuromotor function and falls in chronic stroke. Medicine and Science in Sports and Exercise. 2012; 44: 1409–1418. https://doi.org/10.1249/MSS.0b013e31824e4f8c.

[33] de Oliveira Manoel AL, Macdonald RL. Neuroinflammation as a Target for Intervention in Subarachnoid Hemorrhage. Frontiers in Neurology. 2018; 9: 292. https://doi.org/10.3389/fneur.2018.00292.

[34] Kooijman E, Nijboer CH, van Velthoven CTJ, Mol W, Dijkhuizen RM, Kesecioglu J, *et al*. Long-term functional consequences and ongoing cerebral inflammation after subarachnoid hemorrhage in the rat. PloS One. 2014; 9: e90584. https://doi.org/10.1371/journal.pone.0090584.

[35] Atangana E, Schneider UC, Blecharz K, Magrini S, Wagner J, Nieminen-Kelhä M, *et al*. Intravascular Inflammation Triggers Intracerebral Activated Microglia and Contributes to Secondary Brain Injury After Experimental Subarachnoid Hemorrhage (eSAH). Translational Stroke Research. 2017; 8: 144–156. https://doi.org/10.1007/s12975-016-0485-3.

[36] Smith JA, Das A, Ray SK, Banik NL. Role of pro-inflammatory cytokines released from microglia in neurodegenerative diseases. Brain Research Bulletin. 2012; 87: 10–20. https://doi.org/10.1016/j.brainresbull.2011.10.004.

[37] Zeiler FA, Thelin EP, Czosnyka M, Hutchinson PJ, Menon DK, Helmy A. Cerebrospinal Fluid and Microdialysis Cytokines in Aneurysmal Subarachnoid Hemorrhage: A Scoping Systematic Review. Frontiers in Neurology. 2017; 8: 379. https://doi.org/10.3389/fneur.2017.00379.

[38] He X, Zeng H, Chen JX. Emerging role of SIRT3 in endothelial metabolism, angiogenesis, and cardiovascular disease. Journal of Cellular Physiology. 2019; 234: 2252–2265. https://doi.org/10.1002/jcp.27200.

[39] You Y, Wang Z. Roles of SIRT3 in aging and aging-related diseases. International Journal of Biological Sciences. 2025; 21: 5135–5163. https://doi.org/10.7150/ijbs.115518.

[40] Koentges C, Bode C, Bugger H. SIRT3 in Cardiac Physiology and Disease. Frontiers in Cardiovascular Medicine. 2016; 3: 38. https://doi.org/10.3389/fcvm.2016.00038.

[41] Ansari A, Rahman MS, Saha SK, Saikot FK, Deep A, Kim KH. Function of the SIRT3 mitochondrial deacetylase in cellular physiology, cancer, and neurodegenerative disease. Aging Cell. 2017; 16: 4–16. https://doi.org/10.1111/acel.12538.

[42] Cheng Y, Zhao A, Li Y, Li C, Miao X, Yang W, *et al*. Roles of SIRT3 in cardiovascular and neurodegenerative diseases. Ageing Research Reviews. 2025; 104: 102654. https://doi.org/10.1016/j.arr.2024.102654.

[43] Huang W, Huang Y, Huang RQ, Huang CG, Wang WH, Gu JM, *et al*. SIRT3 Expression Decreases with Reactive Oxygen Species Generation in Rat Cortical Neurons during Early Brain Injury Induced by Experimental Subarachnoid Hemorrhage. BioMed Research International. 2016; 2016: 8263926. https://doi.org/10.1155/2016/8263926.

[44] Zhang K, Cheng H, Song L, Wei W. Inhibition of the Peroxisome Proliferator-Activated Receptor gamma Coactivator 1-alpha (PGC-1α)/Sirtuin 3 (SIRT3) Pathway Aggravates Oxidative Stress After Experimental Subarachnoid Hemorrhage. Medical Science Monitor: International Medical Journal of Experimental and Clinical Research. 2020; 26: e923688. https://doi.org/10.12659/MSM.923688.

[45] Sundaresan NR, Gupta M, Kim G, Rajamohan SB, Isbatan A, Gupta MP. Sirt3 blocks the cardiac hypertrophic response by augmenting Foxo3a-dependent antioxidant defense mechanisms in mice. The Journal of Clinical Investigation. 2009; 119: 2758–2771. https://doi.org/10.1172/JCI39162.

[46] Lanza IR, Short DK, Short KR, Raghavakaimal S, Basu R, Joyner MJ, *et al*. Endurance exercise as a countermeasure for aging. Diabetes. 2008; 57: 2933–2942. https://doi.org/10.2337/db08-0349.